Structural and optical characteristics

by Rajagukguk

Journal of Molecular Structure 1121 (2016) 180–187

Contents lists available at ScienceDirect

Journal of Molecular Structure

journal homepage: http://www.elsevier.com/locate/molstruc

Structural and optical characteristics of Eu^{3+} ions in sodium-lead-zinc-lithium-borate glass system

J. Rajagukguk [a, b], J. Kaewkhao [c, *], M. Djamal [a], R. Hidayat [a], Suprijadi [a], Y. Ruangtaweep [c]

[a] Department of Physics, Faculty of Mathematics and Natural Sciences, Institut Teknologi Bandung, 40132, Indonesia
[b] Department of Physics, Faculty of Mathematics and Natural Sciences, Universitas Negeri Medan, 20221, Indonesia
[c] Center of Excellence in Glass Technology and Materials Science, Nakhon Pathom Rajabhat University, Nakhon Pathom, 73000, Thailand

ARTICLE INFO

Article history:
Received 11 February 2016
Received in revised form
10 May 2016
Accepted 14 May 2016
Available online 17 May 2016

Keywords:
Amorphous glass
Luminescence
Optical properties

ABSTRACT

Structural and optical properties of Eu^{3+}-doped sodium-lead-zinc-lithium-borate glasses $(65-x)B_2O_3-15Na_2O-10PbO-5ZnO-5Li_2O-xEu_2O_3$ (where x = 0, 0.05, 0.1, 0.5, 1.0, 2.0 and 4.0) have been measured and analyzed by varying the Eu^{3+} ion concentrations. The physical parameters such as polaron radius, field strength and inter nuclear distance have been determined from measurements of densities and refractive indices. The structural properties of the prepared borate glasses were analyzed based on X-ray diffraction (XRD) and FTIR instruments. The diffraction spectra show no characteristic peaks in these glasses, which indicates the amorphous nature of the glasses. The infrared spectrum of the Eu^{3+}-doped sodium-lead-zinc-lithium-borate glass systems show three disparate regions for active absorption band around 830–860 cm^{-1}, 1020–1040 cm^{-1} and 1150–1180 cm^{-1}. The electronic transitions in the UV–vis and NIR regions are assigned to the $^7F_0 \rightarrow {}^5D_4$, $^7F_0 \rightarrow {}^5G_2$, $^7F_0 \rightarrow {}^5L_6$, $^7F_0 \rightarrow {}^5D_3$, $^7F_0 \rightarrow {}^5D_2$, $^7F_0 \rightarrow {}^5D_1$, $^7F_0 \rightarrow {}^5D_0$ $^7F_1 \rightarrow {}^5D_0$ $^7F_0 \rightarrow {}^7F_6$ and $^7F_1 \rightarrow {}^7F_6$ levels centered at 362 nm, 380 nm, 395 nm, 414 nm, 465 nm, 533 nm, 583 nm, 590 nm 2092 nm and 2202 nm respectively. Five transition bands of luminescence spectra have been observed by using an excited wavelength of 395 nm. The luminescence intensity ratio (R) of $^5D_0 \rightarrow {}^7F_2$ (electric dipole) transition to $^5D_0 \rightarrow {}^7F_1$ (magnetic dipole) transition has been determined to obtain the strength of the covalent/ionic bond between the Eu^{3+} ions and the surrounding ligands. Radiative life time and emission color of the glasses were estimated and compared with other literature data by varying Eu^{3+} concentrations. The experimental lifetime of the $^5D_0$ level was found to increase with increasing Eu^{3+} ion content, suggesting higher non-radiative energy transfer among Eu^{3+} ions in the glasses.

1. Introduction

Rare-earth (RE) ions in glass structures have been widely investigated with respect to their physical, structural, thermal, electrical and optical properties. During the last decade, RE-doped glasses have become an interesting subject for research because of their potential applications in the fields of photonics, optoelectronics and quantum electronics [1,2].

Among the rare-earth ions, europium (Eu^{3+})-doped glasses receive special attention as optically active glasses. This is because Eu^{3+} ion has a high sensitivity to the local environment generate red luminescence, narrow fluorescence band and long excited state lifetime [3]. Moreover, Eu^{3+}-activated luminescence glasses have been developed for new optical devices, such as solid state lasers, white light emitting diodes (LEDs), plasma display panel (PDP) and emission technology [4]. The local surroundings of RE ions in various crystals and host matrices have been estimated with the help of Eu^{3+} ions emission spectra. Conversely, the local structure of Eu^{3+} has been estimated by using the emission intensity ratio of magnetic dipole ($^5D_0 \rightarrow {}^7F_1$) and forced electric dipole ($^5D_0 \rightarrow {}^7F_2$) transitions [5,6].

Sodium-borate glasses have also been employed extensively as host matrices of lanthanide ions due to their special physical properties, such as high transparency, high thermal stability, low melting point and good rare-earth ion solubility [1,7,8]. Accordingly, sodium oxide (Na_2O) has been added to increase the homogenization and reduce the melting point, of the host glass as well as decrease damages and bubbles. In addition, the presence of

* Corresponding author.
E-mail address: mink110@hotmail.com (J. Kaewkhao).

http://dx.doi.org/10.1016/j.molstruc.2016.05.048
0022-2860/

PbO in some glass compositions matrices is known to improve their stability and visible transparency. Likewise, the addition of PbO and ZnO to the host glass matrices can help to avoid undesirable low durability and thus enhance optical properties, such as higher transmittance in the UV region [9]. On a related note, zinc-borate glasses doped with trivalent europium have been recently studied due to the large direct optical gap of ZnO, which can function as sensitizer for rare-earth ions [10].

Many studies have been carried out to investigate the red light emission properties of Eu^{3+} ion-doped zinc-sodium-lithium-borate glasses [3,8]. Structural and optical properties of Eu^{3+} in lithium-borate glass systems have also been studied by many researchers [11,12]. Several attempts have even succeeded to alter the structural and optical elements in sodium-borate glasses with varying Eu^{3+} ion compositions. Moreover, luminescent studies of the Eu^{3+} (less than 4 mol.%) -doped sodium-borate glass systems were reported [13–15]. Among several emission transitions, the $^5D_0 \rightarrow {}^7F_2$ at 615 nm is known to produce red light luminescence under blue and UV light excitations [16].

This paper aims to investigate the structural and optical characteristics of Eu^{3+} ions in sodium-lead-zinc-lithium-borate glass systems with widely variation of Eu^{3+} up to 4.0 mol.%. The calculation steps on optical properties and Commission Internationale de l'Éclairage (CIE) chromaticity were reported in this work. The effect of concentration quenching on luminescence intensity have been also investigated in this work.

2. Methodology

This paper made use of a Eu^{3+}-doped sodium-lead-zinc-lithium-borate glass as a host matrix. The chemical composition (in mol.%) of the glass host is as follows:

$$(65-x)B_2O_3-15Na_2O-10PbO-5ZnO-5Li_2O-xEu_2O_3$$

where $x = 0$, 0.05, 0.1, 0.5, 1.0, 2.0 and 4.0; the compounds are referred to as 0.0_Eu, 0.05_Eu, 0.1_Eu, 0.5_Eu, 1.0_Eu, 2.0_Eu and 4.0_Eu respectively.

About 20 g of the batch of chemical powders were weighed and thoroughly mixed in an aluminum crucible. The glass samples were prepared by conventional melting-quenching method in an electrical furnace at 1100 °C for 4 h. Furthermore, the melted sample was poured onto a stainless steel plate to be molded into the desired shape. The glasses were then annealed to room temperature in a different furnace at 350 °C for 3 h. The glasses obtained were subsequently cut and polished in order to reach the optimum size for optical measurements to be obtained. The glasses were cut into a dimension of: 10 mm × 10 mm × 3 mm for further treatment.

The glass density (ρ) was measured by means of Archimedes' principle with pure water as immersion liquid:

$$\rho = \frac{w_a}{(w_a - w_l)}\rho_l \quad (1)$$

where w_a and w_l represent the weight of the glass in air and water respectively, and ρ_l is the density of the water (~0.9982 gr/cm^3). To ensure accuracy, each measurement was repeated three times per glass.

The refractive index was measured using an Abbe refractometer with 1-bromonaphthaline as adhesive coating with an accuracy of ±0.001.

Molar volume (V_M) was computed according to the formula:

$V_M = M_T/\rho$, where MT is the molar mass of the sample.

The molar refractivity (R_m) was calculated by utilizing the refractive index and density values following the Volf, Lorentz and Lorenz formula [17]:

$$R_m = \frac{(n^2-1)}{(n^2+2)}\frac{M_T}{\rho} \quad (2)$$

The Eu^{3+} ion concentration (N) was then determined using this formula:

$$N\left(ion/cm^3\right) = \frac{A \cdot N_A \cdot \rho}{M_T} \quad (3)$$

where A is the mole fraction of the RE ions (mol.%) and N_A is Avogadro's number.

After the polish treatment, UV–Vis–NIR Spectrophotometer (Shimadzu UV-3600 model) was used to record the absorption spectra at room temperature. To investigate the glass phase and amorphous visuals of the glass were measured using X-ray diffraction (Shimadzu XRD-6100 model).

The absorption coefficient, $\alpha(\lambda)$, was computed from the equation:

$$\alpha(\lambda) = \frac{1}{d}\ln\frac{I_0}{I} \quad (4)$$

where d is thickness of the glass, I_0 and I are the incident and transmitted radiation intensities respectively.

The direct and indirect transitions of optical band gaps were used to determine the nature of electronic band transition of the absorption. The optical band gap (E_{opt}) was obtained via the following equation [18]:

$$\alpha(\lambda)h\nu = B(h\nu - E_{opt})^n \quad (5)$$

where B is a constant, $h\nu$ is the photon energy of incident radiation and n is an index number (n = ½ and n = 2 for direct and indirect transitions respectively).

The infrared spectra were measured using Agilent Technologies Cary 630 Fourier Transform Infrared (FTIR) spectrometer in the range of 500–3000 cm^{-1}. Emission spectra of the Eu^{3+}-doped-sodium-borate glasses were measured using Agilent Technologies Eclipse Fluorescence spectrophotometer in the wavelength range of 500–750 nm.

Excitation wavelength at 395 nm ($^7F_0 \rightarrow {}^5L_6$ band) was chosen to record the emission spectra and their decay times using arc xenon lamp at 500–750 nm. All measurements were recorded at room temperature.

Several other physical properties of the glasses, such as polaron radius (r_i), internuclear distance (r_p), field strength (F), dielectric constant (ε) and polarizability of oxide ions (α_m) of the Eu^{3+} glasses were investigated by means of general formulae [19–22] (see Table 1).

3. Results and discussion

All the physical properties of the different glass compounds as previously measured and calculated are presented in Table 2.

The densities of the glass compounds were found to have increased slightly with the increase in Eu^{3+} concentration from 0.05 mol% of Eu^{3+} to 4.0 mol%, exhibiting a linear relationship. This increase can be attributed to the B_2O_3 ions which were replaced by Eu^{3+} ions, whose higher molecular mass. The content of Eu_2O_3 is found to be able to modify the glass network because the density of the glass depends on the compactness of its structure, changes in its geometrical configuration, cross-link density, coordination number and the interstitial sites within itself [23]. In our samples,

Table 1
Initials and the respective chemical compositions of the observed samples.

No	Glass initial	B_2O_3 (mol%)	Na_2O (mol%)	PbO (mol%)	ZnO (mol%)	Li_2O (mol%)	Eu_2O_3 (mol%)
1	0.0_Eu	65.00	15.0	10.0	5.0	5.0	–
2	0.05_Eu	64.95	15.0	10.0	5.0	5.0	0.05
3	0.1_Eu	64.90	15.0	10.0	5.0	5.0	0.10
4	0.5_Eu	64.50	15.0	10.0	5.0	5.0	0.50
5	1.0_Eu	64.00	15.0	10.0	5.0	5.0	1.00
6	2.0_Eu	63.00	15.0	10.0	5.0	5.0	2.00
7	4.0_Eu	61.00	15.0	10.0	5.0	5.0	4.00

Table 2
Physical properties of Eu^{3+}-doped sodium-lead-zinc-lithium-borate glasses.

Physical properties	Glass samples						
	0.0_Eu	0.05_Eu	0.1_Eu	0.5_Eu	1.0_Eu	2.0_Eu	4.0_Eu
Molar weight, M (g)	82.43	82.57	82.72	83.85	85.26	88.08	93.73
Density, ρ (g/cm^3)	2.98	2.89	2.90	2.93	2.96	3.03	3.15
Molar volume, M_V (cm^3/mol)	27.65	28.54	28.54	28.54	28.60	29.05	29.74
Ion concentration, N (x10^{22} ion/cm^3)	0.00	0.11	0.21	1.05	2.09	4.15	8.11
Polaron radius, r_i (Å)	–	3.956	3.14	1.838	1.463	1.164	0.931
Inter nuclear distance, r_p (Å)	–	9.818	7.792	4.56	3.629	2.89	2.31
Field strength, F (x10^{16} cm^{-2})	–	1.577	2.503	7.309	11.54	18.22	28.48
Refractive index, n	1.531	1.535	1.572	1.575	1.597	1.600	1.604
Optical band gap, E_g	3.007	2.951	3.002	3.070	3.058	3.006	3.009
Dielectric constant, ε	5.736	5.81	5.44	5.657	5.672	5.738	5.734
Molar refractivity, R_m (cm^{-3})	16.93	17.58	17.48	17.39	17.563	17.79	18.21
Polarizability of oxide ions, α_m ($\times 10^{-24}$ cm^3)	6.711	6.969	6.931	6.895	6.962	7.052	7.217

the relative molecular mass of Eu_2O_3 was 351.93 g and that of B_2O_3 was 69.62 g, indicating that the increase of Eu_2O_3 concentration is directly at the expense of B_2O_3, which causes an increase of relative density.

Molar volume of the glasses is also an important physical property of the samples. As can be seen from Fig. 1, the molar volume of the glasses increases with increasing composition of Eu^{3+}. The increase of molar volume with the addition of Eu^{3+} ions affected by the rates of density change and molecular weight of Eu^{3+} ion. When Eu^{3+} ion added into the glass network, then there was a position transformation from network modifier former to network modifier. This indicates that the number of non-bridging oxygen (NBO) has increased [24,25]. Although density and molar volume are inversely proportional in theory, the data suggests that both parameters increase with an increase in Eu^{3+} concentration.

The X-ray diffraction (XRD) patterns of the sodium-lead-zinc-lithium-borate glasses are shown in Fig. 2. The analysis of the XRD data shows no sharp diffraction peak, but a broad hump can be observed around 28° (2θ), reflecting a characteristic of amorphous material. This indicates that the Eu^{3+} in sodium-lead-zinc-lithium-borate glasses have an amorphous state behavior.

Fig. 3 shows the infrared spectra, identifying the functional groups of the Eu^{3+}-doped sodium-borate glass system. All the spectral measurements were of a range of 600–1500 cm^{-1}, and were assigned to asymmetric vibration modes of the borate network. Generally, there are three disparate regions for the active absorption band in the borate glass network. The first region is attributed to the B–O stretching vibration of the trigonal (BO_3) unit, which lies at the 1100–1700 cm^{-1} range. The second group is

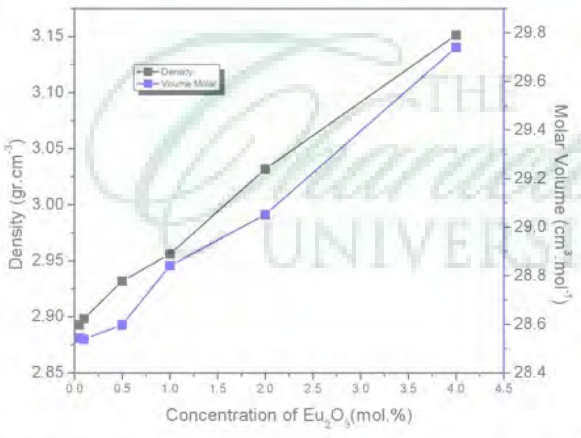

Fig. 1. Density and molar volume of glass compounds for differing values of Eu^{3+} concentration.

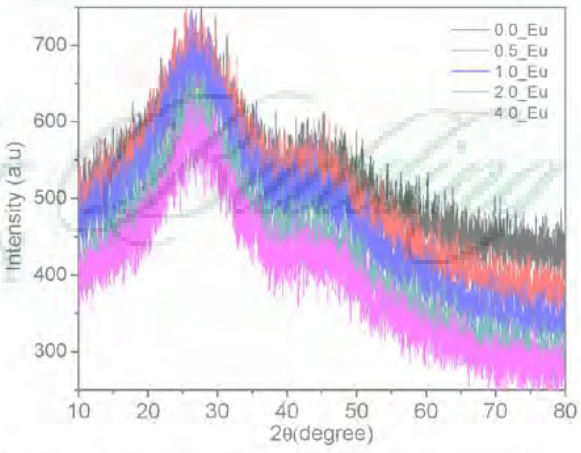

Fig. 2. X-ray diffraction pattern of Eu^{3+}-doped sodium-lead-zinc-lithium-borate glass system.

assigned to the B–O bond stretching of the tetrahedral (BO_4) unit observed at around 800–1100 cm^{-1}. The third region observed in the range 400–800 cm^{-1} is assigned to the bending vibration of B–O–B linkages in the borate network [26–28]. As presented in Fig. 3, the absorption bands are found around 830–860 cm^{-1}, 1020–1040 cm^{-1} and 1170–1180 cm^{-1}. The absorption peak found around 830–860 cm^{-1} can be assigned to the symmetric stretching vibrations of B–O bonds and B–O–B bending vibrations from diborate groups and BO_4 groups respectively [29]. The peak around 1170–1180 cm^{-1} may be due to the BO_4 stretching vibration in the pyroborate groups.

To identify the optical transition of the Eu^{3+}-doped sodium-lead-zinc-lithium-borate glass, the absorption spectra measurements for 2.0_Eu sample were carried out at room temperature in the wavelength range of 350–2300 nm as shown in Fig. 4. The assignments of the absorption spectra exhibit a maximum 10 transition bands derived from the ground state $^7F_0$ and the first excited state $^7F_1$. The absorption spectral bands that originate from $^7F_1$ and $^7F_2$ were predicted to appear due to these transitions being closely located to the $^7F_0$ ground state. However, transitions originating from the $^7F_2$ level were too weak to be investigated because of the minimum fractional thermal populations [30,31]. Moreover, the absorption band positions in the glass samples are similar to those reported in other literature, with only small differences in the peak positions [1–16].

The electronic transitions in the UV–Vis regions are assigned to the $^7F_0 \rightarrow {}^5D_4$, $^7F_0 \rightarrow {}^5G_2$, $^7F_0 \rightarrow {}^5L_6$, $^7F_0 \rightarrow {}^5D_3$, $^7F_0 \rightarrow {}^5D_2$, $^7F_0 \rightarrow {}^5D_1$, $^7F_0 \rightarrow {}^5D_0$ and $^7F_1 \rightarrow {}^5D_0$ levels, centered at 362 nm, 380 nm, 395 nm, 414 nm, 465 nm, 533 nm, 583 nm and 590 nm respectively. Conversely, the transitions in the NIR region correspond to $^7F_0 \rightarrow {}^7F_6$ and $^7F_1 \rightarrow {}^7F_6$ levels, with wavelength peaks at 2092 nm and 2202 nm respectively. The transition assignment of the Eu^{3+} absorption bands has been adjusted on the earlier reports [3,4,32]. In the case of Eu^{3+}-doped sodium-lead -zinc-lithium-borate glasses, the absorption band corresponding to $^7F_0 \rightarrow {}^5L_6$ transition is more intense than all other absorption transitions. In addition, this transition is forbidden by the ΔS and ΔL selection rules, but is not by the ΔJ selection rule [3]. Furthermore, the intensity of the $^7F_0 \rightarrow {}^5D_2$ (electric dipole) transition was observed to be higher than that of the $^7F_0 \rightarrow {}^5D_1$ transition (magnetic dipole), such that the $^7F_0 \rightarrow {}^5D_2$ transition is commonly referred to as hypersensitive transition [33,34]. Our glass samples show that the absorption intensity of the $^7F_0 \rightarrow {}^5D_0$ transition is relatively very weak because of the forbidden spin as followed by the $^7F_0 \rightarrow {}^5D_{J(J=0,1,2,3,4)}$ absorption and emission bands. On the other hand, the absorption intensity for the $^7F_0 \rightarrow {}^5D_3$ transition could not be observed in the spectra of the Eu^{3+}-doped sodium-borate system glass, as it is not allowed by the $\Delta J = 3$ selection rule.

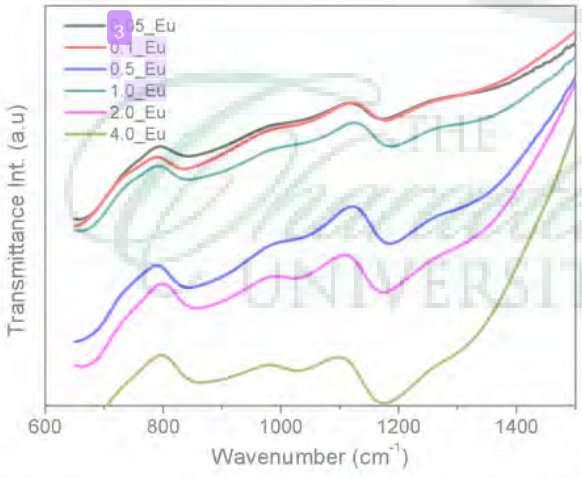

Fig. 3. Infrared spectra of the glass compounds for differing values of Eu^{3+} concentration.

According to the Davis and Mott theory, the optical band gaps (E_{opt}) for both direct and indirect transitions can be determined from the relationship between the absorption coefficient, $\alpha(\lambda)$ and photon energy, $h\nu$, as shown in Eq. (5). Fig. 5a and b shows the relationship between the direct and indirect optical band gaps respectively for all of glass sample. The optical band gap magnitudes of the different glass samples were computed by extrapolating the linear region of the curves to the $h\nu$ axis. A more comprehensive list is given in Table 3.

It can be observed that the optical band gap strongly depends on the Eu^{3+} composition. The optical band gap energies exist in the range of 3.47–3.60 eV for the direct transition and 2.95–3.07 eV for the indirect transition. From Table 3, it can be seen that the smallest value of optical band gap is given by the 0.05_Eu sample for both direct and indirect transitions. Furthermore, the optical band gap values are similar for the 0.0_Eu and 0.1_Eu pair, as well as that of 2.0_Eu and 4.0_Eu. In addition, the value of indirect optical band gap decreases slightly as the Eu_2O_3 concentration is increased from 0.5 mol% to 4.0 mol%. This result indicates that the addition of Eu^{3+} to the borate glass system increases the number of non-bridging oxygens (NBO) and affects optical band gap values [35].

The observed emission and excitation spectra of Eu^{3+}-doped sodium-lead-zinc-lithium-borate glasses are shown in Fig. 6 and Fig. 7 respectively. The observed excitation spectra are found to be similar to the resulted absorption spectra and were consistent with the other reported Eu^{3+}-doped glasses [33–36]. The excitation spectrum of the 2.0 mol% Eu^{3+}-doped glass composition was recorded using the prominent emission transition of $^5D_0 \rightarrow {}^7F_2$ at 615 nm. The various excitation transitions are assigned to $^7F_0 \rightarrow {}^5H_6$, $^7F_0 \rightarrow {}^5D_4$, $^7F_0 \rightarrow {}^5L_7$, $^7F_0 \rightarrow {}^5L_6$, $^7F_0 \rightarrow {}^5D_3$, $^7F_0 \rightarrow {}^5D_2$, $^7F_0 \rightarrow {}^5D_1$, $^7F_0 \rightarrow {}^5D_0$, and $^7F_1 \rightarrow {}^5D_0$ levels with the wavelength peaks at 320, 363, 381, 395, 414, 465, 533, 578 and 588 nm respectively. The $^7F_0 \rightarrow {}^5L_6$ and $^7F_0 \rightarrow {}^5D_2$ transitions are relatively high intensities compared to the other transitions. This indicates that the excitation light at 395 nm and 463 nm are efficient pumping sources which can stimulate a higher number of atoms to generate Eu^{3+} luminescence.

Fig. 6 shows emission spectra for 0.05_Eu, 0.1_Eu, 0.5_Eu, 1.0_Eu, 2.0_Eu and 4.0_Eu glasses from 500 to 750 nm range under excitation sources by arc xenon lamp at 395 nm. Five emission bands in the visible range have been recorded from ground state $^5D_0$ to $^7F_0$, $^7F_1$, $^7F_2$, $^7F_3$, $^7F_4$ with the wavelength peaks corresponding to 577 nm, 590 nm, 613 nm, 651 nm and 700 nm respectively. It can been seen that the $^5D_0 \rightarrow {}^7F_2$ transition appears to have the highest emission intensity that follows the selection rule $\Delta J = 2$. A weak emission band located at the $^5D_0 \rightarrow {}^7F_0$ transition suggests that the surroundings of the Eu^{3+} ions possess higher asymmetry in the glass materials [34,37]. The emission phenomena of these glass systems have been confirmed and are of similar characteristics to those of several other works [4,11,13,15]. However there is a difference in luminescence concentration quenching for each paper reported.

Among all glass samples, the 2.0_Eu glass shows the strongest intensity for each emission band transitions shows strong red emission. The addition of Eu^{3+} dopant from 0.05 mol% to 2.0 mol% increases the emission intensities, although it then decreases drastically when Eu^{3+} content is 4.0 mol% due to the interactions among the dipole pair in the energy level manifolds as well as cross relaxation processes [2].

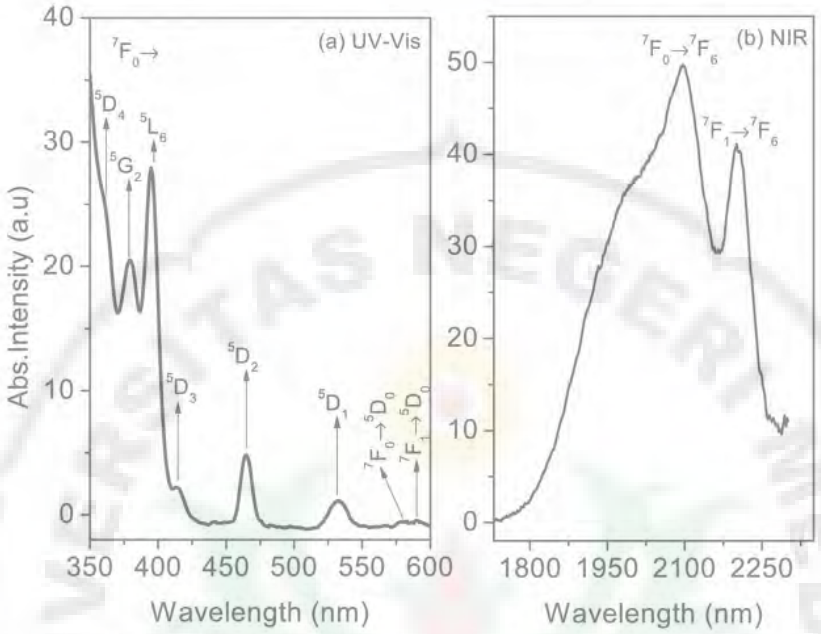

Fig. 4. Optical absorption spectra of 2.0 mol.% Eu^{3+} in borate glass in: (a) UV-VIS region and (b) NIR region.

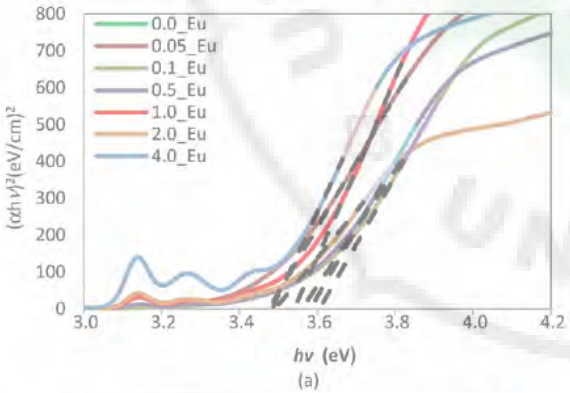

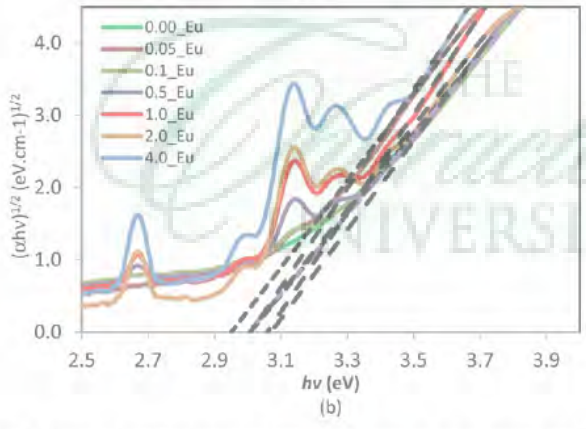

Fig. 5. Direct and indirect band gap energies of sodium-lead-zinc-lithium-borate glasses.

Table 3
Direct and indirect optical band gaps of the various glass samples.

No	Glasses	Optical band gap (eV)	
		Direct	Indirect
1	Pure	3.56	3.00
2	0.05_Eu	3.47	2.95
3	0.1_Eu	3.60	3.00
4	0.5_Eu	3.58	3.07
5	1.0_Eu	3.54	3.05
6	2.0_Eu	3.49	3.01
7	4.0_Eu	3.48	3.01

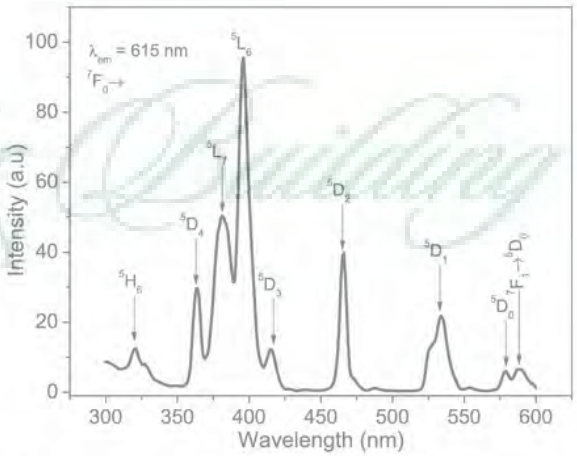

Fig. 6. Excitation spectra (λ_{em} = 615 nm) of the 2.0 mol% Eu^{3+} ion-doped glass system.

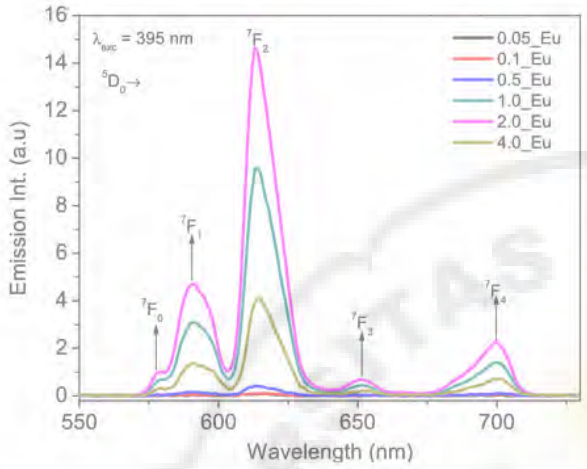

Fig. 7. Luminescence spectra (λ_{exc} = 395 nm) of the different Eu^{3+}-doped sodium-lead-zinc-lithium-borate glass samples.

Luminescence quenching of the Eu^{3+}-doped sodium-lead-zinc-lithium-borate glass system was observed for Eu^{3+} concentration more than 2.0 mol.%. The effects of Eu^{3+} on the luminescence spectra have been studied by K. Maheshvaran et al. [37]. It is reported that concentration quenching observed at 3.0 mol% and luminescence intensity of Eu^{3+} increases with the concentration of Eu_2O_3, increasing for 0.01; 0.1; 1.0 and 2.0 mol%. These results are consistent to those of our glass samples, for which the most intense luminescence occurs at 2.0 mol%. Karunakaran et al., (lithium-fluoroborate glasses) [13] and Vijayakumar et al., (telluro-fluoroborate glasses) [38] also reported that the luminescence intensity of Eu^{3+}-doped glasses increases 1.0–2.0 mol%, then decreasing beyond 2.0 mol% due to concentration quenching. On the other hand, Kiran et al. [3], reported that no concentration quenching was observed in Eu^{3+}-doped lead-alkali-fluoroborate glasses, with the most intense luminescence occurring at 2.0 mol%.

The luminescence intensity ratio (R) of the $^5D_0 \rightarrow {}^7F_2$ (electric dipole) transition to the $^5D_0 \rightarrow {}^7F_1$ (magnetic dipole) transition has been determined and the results are shown in Table 4. This parameter was used to obtain the strength of the covalent/ionic bond between the Eu^{3+} ions and the surrounding ligands. The luminescence intensity ratio is relatively increase with content of Eu_2O_3 up to 1.0 mol%. Then decrease up to 3.03 for 4.0 mol% Eu^{3+}. Increase of luminescence intensity ratio indicates a higher asymmetry around the Eu^{3+} ions in the glass samples and also reflects stronger covalent bonds between the Eu^{3+} ions and the surrounding ligands. Conversely, decrease of R is defined as higher the symmetry around the Eu^{3+} ions and the covalence of Eu- O is lower [39].

As seen in Fig. 8, Eu^{3+} ions were pumped to up levels. A fast non radiative (NR) multiphonon relaxation from excited state to the $^5D_0$ level results in emission transitions corresponding to $^5D_0 \rightarrow {}^7F_J$ (J = 0, 1, 2, 3, 4). Moreover, the emission bands from $^5D_1$, $^5D_2$ and $^5D_3$ levels are negligible compared to emission from the $^5D_0$ level because of the high energy phonons in the glass materials [40].

Table 4
$^5D_0 \rightarrow {}^7F_2/{}^5D_0 \rightarrow {}^7F_1$ luminescence intensity ratios (R).

Intensity ratio	Eu^{3+} Initial glass					
	0.05_Eu	0.1_Eu	0.5_Eu	1.0_Eu	2.0_Eu	4.0_Eu
$^5D_0 \rightarrow {}^7F_2/{}^5D_0 \rightarrow {}^7F_1$	1.87	2.08	2.46	3.11	3.07	3.03

The Commission Internationale de l'Éclairage (CIE) chromaticity diagram of six Eu^{3+}-doped sodium-borate glasses upon 395 nm excitations is shown in Fig. 9. The emission spectra are used to calculate the color coordinates in X–Y axis for the following configurations: $x = 0.57$ and $y = 0.42$ for 0.05 mol% Eu^{3+}; $x = 0.54$ and $y = 0.44$ for 0.1 mol% Eu^{3+}; $x = 0.62$ and $y = 0.38$ for 0.5 mol% Eu^{3+}; $x = 0.65$ and $y = 0.35$ for 1.0 mol% Eu^{3+}; $x = 0.65$ and $y = 0.35$ for 2.0 mol% Eu^{3+}; $x = 0.64$ and $y = 0.35$ for 4.0 mol% Eu^{3+}. The emission light color can be seen to shift from orange to red as the Eu^{3+} ion concentration increases up 4.0 mol%.

The emission decay time of the $^5D_0 \rightarrow {}^7F_2$ transition at 615 nm of the different glass samples is shown in Fig. 10. The measured lifetime values were carried out under excitation at 395 nm in order to obtain further information about luminescence radiative properties of Eu^{3+}-doped sodium-lead-zinc-lithium-borate glass systems. The decay shapes were adjusted according to the first order exponential equation because the non-radiative multiphonon relaxation was the dominant transition. Decay time is observed to increase with increasing Eu^{3+} ion concentrations from 0.05_Eu to 4.0_Eu as seen in Table 5. The glass sample with 0.05_Eu label shows the shortest luminescence life time of about 1.7 ms compared to the other glasses that were recorded. The longest luminescence life time is achieved by the 4.0_Eu glass for around 6.1 ms, slightly longer than the Eu^{3+}-doped FPO3 glass as reported in another study [41]. The increase of the experimental lifetime did not occur significantly following the rise of the Eu^{3+} concentration. This shows that the experimental lifetime dominantly depends on host material composition.

4. Conclusion

In conclusion, this paper investigates the structural and optical properties of Eu^{3+} ions in a novel glass material based on sodium-lead-zinc-lithium-borate composition, in order to determine the optimum concentration value. It was found that the concentration dopant at 2.0 mol.% can generate the highest luminescence intensity compared with other Eu^{3+} concentrations. The diffraction spectra of the samples show no characteristic peaks in these glasses

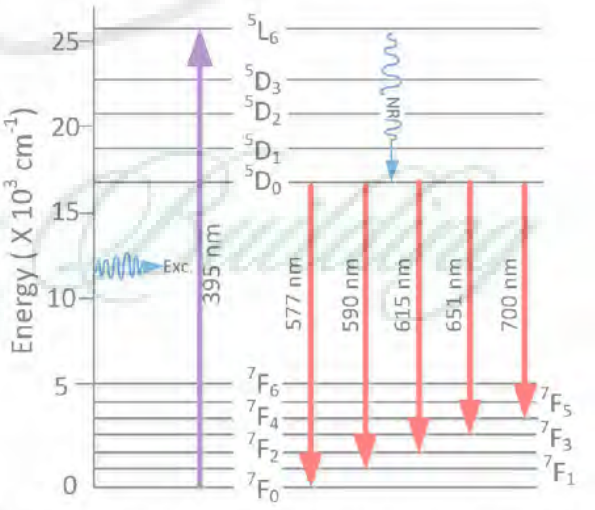

Fig. 8. Energy level diagram for excitation and emission transitions of Eu^{3+} in borate glass system by 395 nm photon wavelength.

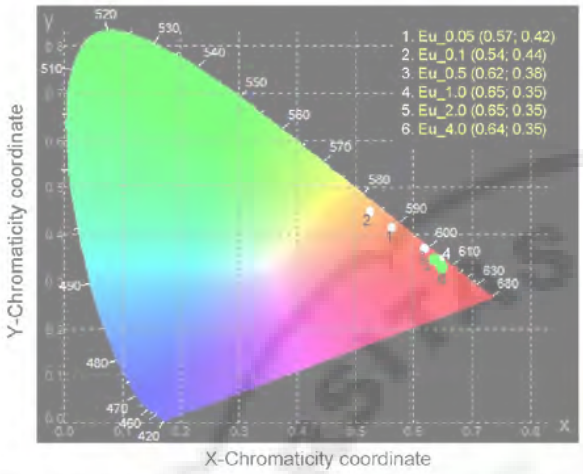

Fig. 9. Diagram of CIE chromaticity for Eu^{3+} ion-doped borate glass systems CIE = Commission Internationale de l'Éclairage.

after addition of Eu^{3+} dopant, which indicates the glasses still amorphous phase nature. Moreover, the Infrared spectrum of the glass system shows three disparate regions for an active absorption band around 830–860 cm^{-1}, 1020–1040 cm^{-1} and 1170–1180 cm^{-1}. The electronic transitions in the UV–Vis and NIR regions are found to be assigned to the $^7F_0 \rightarrow {}^5D_4$, $^7F_0 \rightarrow {}^5G_2$, $^7F_0 \rightarrow {}^5L_6$, $^7F_0 \rightarrow {}^5D_3$, $^7F_0 \rightarrow {}^5D_2$, $^7F_0 \rightarrow {}^5D_1$, $^7F_0 \rightarrow {}^5D_0$ $^7F_1 \rightarrow {}^5D_0$ $^7F_0 \rightarrow {}^7F_6$ and $^7F_1 \rightarrow {}^7F_6$ levels centered at 362 nm, 380 nm, 395 nm, 414 nm, 465 nm, 533 nm, 583 nm, 590 nm 2092 nm and 2202 nm respectively. Furthermore, five transition bands of luminescence spectra have been observed using an excited wavelength of 395 nm. Lastly, decay time is found to increase slightly with increasing Eu^{3+} ion concentrations from 0.05_Eu to 4.0_Eu, declared that experimental lifetime depend on composition of the host glass material.

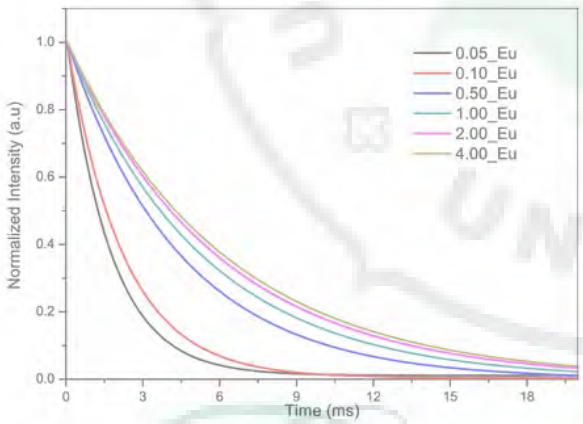

Fig. 10. Decay rates for $^5D_0 \rightarrow {}^7F_2$ transition of Eu^{3+}-doped sodium-lead-zinc-lithium-borate glasses.

Table 5
Measured lifetimes for $^5D_0 \rightarrow {}^7F_2$ transition of Eu^{3+}-doped sodium-borate glass systems.

Eu^{3+} Initial glass	Lifetime (ms)	References
0.05_Eu	1.709	Present work
0.1_Eu	2.182	Present work
0.5_Eu	4.425	Present work
1.0_Eu	5.249	Present work
2.0_Eu	5.826	Present work
4.0_Eu	6.103	Present work
Eu3+:LBTAF	1.28	[34]
Eu3+:Glass-A	1.984	[40]
Eu3+:PbO–TeO2	0.64	[41]
Eu3+:PbO–SiO2	1.27	[41]
Eu3+:FP03	6.0	[42]

References

[1] S. Arunkumar, K.V. Krishnaiah, K. Marimuthu, Structural and luminescence behavior of lead fluoroborate glasses containing Eu^{3+} ions, Phys. B Phys. Cond. Matter 416 (2013) 88–100, http://dx.doi.org/10.1016/j.physb.2013.02.022.

[2] B.D. Prasad, C.M. Reddy, Structural and optical investigations of Eu^{3+} ions in lead containing alkali fluoroborate glasses, Opt. Mat. 34 (8) (2012) 1251–1260, http://dx.doi.org/10.1016/j.optmat.2012.01.027.

[3] N. Kiran, Eu^{3+} ion doped sodium – lead borophosphate glasses for red light emission, J. Mol. Struct. 1065–1066 (2014) 93–98, http://dx.doi.org/10.1016/j.molstruc.2014.02.047.

[4] K. Swapna, S. Mahamuda, A.S. Rao, T. Sasikala, P. Packiyaraj, L.R. Moorthy, G.V. Prakash, Luminescence characterization of Eu^{3+} doped Zinc Alumino Bismuth Borate glasses for visible red emission applications, J. Lumin. 156 (2014) 80–86, http://dx.doi.org/10.1016/j.jlumin.2014.07.022.

[5] Y. Yang, Z. Ren, Y. Tao, Y. Cui, H. Yang, Eu^{3+} emission in $SrAl_2B_2O_7$ based phosphors, Curr. App. Phys. 9 (3) (2009) 618–621, http://dx.doi.org/10.1016/j.cap.2008.05.015.

[6] Hongli Wen, Guohua Jia, Chang-Kui Duan, Peter A. Tanner, Understanding Eu^{3+} emission spectra in glass, Phys. Chem. Chem. Phys. 12 (33) (2010) 9933–9937, http://dx.doi.org/10.1039/C0CP00206B.

[7] B.D. Prasad, C.M. Reddy, Structural and optical investigations of Eu^{3+} ions in lead containing alkali fluoroborate glasses, Opt. Mater. 34 (8) (2012) 1251–1260, http://dx.doi.org/10.1016/j.optmat.2012.01.027.

[8] J. Anjaiah, C. Laxmikanth, N. Veeraiah, Spectroscopic properties and luminescence behaviour of europium doped lithium borate glasses, Phys. B Phys. Condens. Matter 454 (2014) 148–156, http://dx.doi.org/10.1016/j.physb.2014.07.070.

[9] M.A. Marzouk, F.H. Elbatal, A.M. Abdelghany, Ultraviolet and infrared absorption spectra of Cr_2O_3 doped – sodium metaphosphate, lead metaphosphate and zinc metaphosphate glasses and effects of gamma irradiation : a comparative study, Spectr. Acta Part A Molecular Biomolecular Spectroc. 114 (2013) 658–667, http://dx.doi.org/10.1016/j.saa.2013.05.093.

[10] K. Annapurna, M. Das, P. Kundu, R.N. Dwivedi, S. Buddhudu, Spectral properties of Eu^{3+} :ZnO–B_2O_3–SiO_2 glasses, J. Molecular Struct. 741 (2005) 53–60, http://dx.doi.org/10.1016/j.molstruc.2005.01.062.

[11] M.A.K. Elfayoumi, M. Farouk, Structural properties of Li–borate glasses doped with Sm^{3+} and Eu^{3+} ions, J. Alloys Comp. 482 (2009) 356–360, http://dx.doi.org/10.1016/j.jallcom.2009.04.021.

[12] P.S. Wong, M.H. Wan, R. Hussin, H.O. Lintang, S. Endud, Structural and luminescence studies of europium ions in lithium aluminium borophosphate glasses, J. Rare Earths 32 (7) (2014) 585–592, http://dx.doi.org/10.1016/S1002-0721(14)60112-5.

[13] R.T. Karunakaran, K. Marimuthu, S.S. Babu, S. Arumugam, Structural, optical and thermal studies of Eu^{3+} ions in lithium fluoroborate glasses, Solid State Sci. 11 (11) (2009) 1882–1889, http://dx.doi.org/10.1016/j.solidstatesciences.2009.08.001.

[14] Y. Yang, B. Chen, C. Wang, H. Zhong, L. Cheng, J. Sun, Y. Peng, X. Zhang, Investigation on structure and optical properties of Er^{3+}, Eu^{3+} single-doped PbO – ZnO – B_2O_3–TeO_2 glasses, Opt. Mater. 31 (2008) 445–450, http://dx.doi.org/10.1016/j.optmat.2008.06.014.

[15] Y. Zheng, Y. Qu, Y. Tian, C. Rong, Z. Wang, S. Li, X. Chen, Y. Ma, Effect of Eu^{3+}-doped on the luminescence properties of zinc borate nanoparticles, J. Coll. 349 (2009) 19–22, http://dx.doi.org/10.1016/j.colsurfa.2009.07.039.

[16] Pun, D. Yang, G. Liu, T. Ma, B. Zhai, Q. An, J. Yu, X. Wang, X. Liu, E.Y. Pun, Optical absorption and photoluminescence in Sm^{3+} and Eu^{3+} -doped rare-earth borate glasses, J. Lumin. 113 (2005) 121–128, http://dx.doi.org/10.1016/j.jlumin.2004.09.115.

[17] E.A. Davis, N.F. Mott, Conduction in non-crystalline systems V. Conductivity, optical absorption and photoconductivity in amorphous semiconductors, Philos. Mag. 22 (179) (1970) 0903–0922, http://dx.doi.org/10.1080/14786437008221061.

[18] M. Abdel-Baki, F.A. Abdel-Wahab, A. Radi, F. El-Diasty, Factors affecting optical dispersion in borate glass systems, J. Phys. Chem. Solids 68 (8) (2007) 1457–1470, http://dx.doi.org/10.1016/j.jpcs.2007.03.026.

[19] L.E.O.W. Tingqiao, L.I.U. Hong, R. Hussin, Z. Ibrahim, K. Deraman, H. Lintang, W. Shamsuri, Effects of Eu^{3+} and Dy^{3+} doping or co-doping on optical and structural properties of $BaB_2Si_2O_8$ phosphor for white LED applications, J. Rare Earths 34 (1) (2016) 21–29, http://dx.doi.org/10.1016/S1002-0721(14)60573-8.

[20] M.H.A. Mhareb, S. Hashim, S.K. Ghoshal, Y.S.M. Alajerami, M.A. Saleh,

R.S. Dawaud, S.A.B. Azizan, Impact of Nd^{3+} on physical and optical properties of Lithium Magnesium Borate glass, Opt. Mater. (2014) 1–7, http://dx.doi.org/10.1016/j.optmat.2014.06.033.

[21] W.A.W. Razali, K. Azman, H.J.M. Ridzwan, H. Azhan, S.A. Senawi, M.R. Sahar, M.S. Rohani, Effect of Li_2O on the physical properties of Nd_2O_3 doped tellurite glass, Solid State Sci. Tech. 20 (1–2) (2012) 121–127.

[22] X. Joseph, R. George, S. Thomas, M. Gopinath, M.S. Saina, N.V. Unnikrishnan, Spectroscopic investigations on Eu^{3+} ions in Li – Zn fluorotellurite glasses, Opt. Mater. 37 (2014) 552–560, http://dx.doi.org/10.1016/j.optmat.2014.07.021.

[23] Y.B. Saddeek, K.A. Aly, S.A. Bashier, Optical study of lead borosilicate glasses, Phys. B Condens. Matter 405 (10) (2010) 2407–2412, http://dx.doi.org/10.1016/j.physb.2010.02.055.

[24] P. Chimalawong, J. Kaewkhao, P. Limsuwan, Spectroscopic studies of Nd^{3+} doped soda-lime-silicate glasses, J. Mater. Sci. Eng. B 2 (6) (2012) 363–367.

[25] I. Kashif, S.A. Rahman, A.A. Soliman, E.M. Ibrahim, E.K. Abdel-khalek, A.G. Mostafa, A.M. Sanad, Effect of alkali content on AC conductivity of borate glasses containing two transition metals, Phys. B Condens. Matter 404 (21) (2009) 3842–3849.

[26] S. Arunkumar, K. Marimuthu, Structural and luminescence studies on Eu^{3+}: B_2O_3–Li_2O–MF–LiF (M = Ba, Bi_2, Cd, Pb, Sr_2 and Zn) glasses, J. Lumin. 139 (2013) 6–15, http://dx.doi.org/10.1016/j.jlumin.2013.02.014.

[27] H.A. Othman, H.S. Elkholy, I.Z. Hager, FTIR of binary lead borate glass: structural investigation, J. Mol. Struct. 1106 (2016) 286–290, http://dx.doi.org/10.1016/j.molstruc.2015.10.076.

[28] A. Thulasiramudu, S.A. Buddhudu, Optical characterization of Cu^{2+} ion-doped lead borate glasses, J. Quant. Spectros. Rad. Transf. 97 (2006) 181–194, http://dx.doi.org/10.1016/j.jqsrt.2005.04.006.

[29] A. Balakrishna, D. Rajesh, Y.C. Ratnakaram, Structural and optical properties of Nd^{3+} in lithium fluoro-borate glass with relevant modifier oxides, Opt. Mater. 35 (12) (2013) 2670–2676, http://dx.doi.org/10.1016/j.optmat.2013.08.004.

[30] R. Vijaya, C.K. Jayasankar, Structural and spectroscopic properties of Eu^{3+} doped zinc fluorophosphate glasses, J. Molec. Struct. 1036 (2013) 42–50, http://dx.doi.org/10.1016/j.molstruc.2012.09.037.

[31] K. Marimuthu, R.T. Karunakaran, S.S. Babu, G. Muralidharan, S. Arumugam, C.K. Jayasankar, Structural and spectroscopic investigations on Eu^{3+} doped alkali fluoroborate glasses, Solid State Sci. 11 (7) (2009) 1297–1302, http://dx.doi.org/10.1016/j.solidstatesciences.2009.04.011.

[32] W.T. Carnall, P.R. Fields, K. Rajnak, Electronic energy levels of the trivalent lanthanide aquo ions. IV. Eu3+, J. Chem. Phys. 49 (10) (1968) 4450–4455.

[33] M.M. Mohan, L.R. Moorthy, D. Ramachari, C.K. Jayasankar, Spectroscopic investigation and optical characterization of Eu^{3+} ions in K–Nb–Si glasses, Spectrochim. Acta A 118 (2014) 966–971.

[34] B.C. Jamalaiah, J.S. Kumar, A.M. Babu, L.R. Moorthy, Spectroscopic studies of Eu^{3+} ions in LBTAF glasses, J. Alloys Compd. 478 (2009) 63–67.

[35] T.G.V.M. Rao, A. Rupesh Kumar, K. Neeraja, N. Veeraiah, M. Rami Reddy, Optical and structural investigation of Eu3+ ions in Nd3+ co-doped magnesium lead borosilicate glasses, J. Alloys Compd. 557 (2013) 209–217.

[36] K. Maheshvaran, P.K. Veeran, K. Marimuthu, Structural and optical studies on Eu^{3+} doped boro-tellurite glasses, Solid State Sci. 17 (2013) 54–62.

[37] K. Maheshvaran, K. Marimuthu, Concentration dependent Eu^{3+} doped boro-tellurite glasses — Structural and optical investigations, J. Lumin. 132 (9) (2012) 2259–2267.

[38] R. Vijayakumar, K. Maheshvaran, V. Sudarsan, K. Marimuthu, Concentration dependent luminescence studies on Eu^{3+} doped telluro fluoroborate glasses, J. Lumin. 154 (2014) 160–167.

[39] K. Linganna, C.K. Jayasankar, Optical properties of Eu3+ ions in phosphate glasses, Spectrochim. Acta Part A Mol. Biomol. Spectrosc. 97 (2012) 788–797.

[40] C.H. Kam, S. Buddhudu, Emission analysis of Eu^{3+}: Bi_2O_3–B_2O_3– R_2O (R = Li; Na; K) glasses, J. Quant. Spectros. Rad. Transf. 87 (2004) 325–337, http://dx.doi.org/10.1016/j.jqsrt.2004.03.006.

[41] W.A. Pisarski, J. Pisarska, L. Zur, T. Goryczka, Structural and optical aspects for Eu^{3+} and Dy^{3+} ions in heavy metal glasses based on PbO-Ga_2O_3-XO_2 (X = Te, Ge, Si), Opt. Mater. 35 (2013) 1051–1056, http://dx.doi.org/10.1016/j.optmat.2012.12.012.

[42] A. Herrmann, S. Fibikar, D. Time-resolved fluorescence measurements on Eu^{3+} - and Tb^{3+}-doped glasses, J. Non-Cryst. Solids 355 (43–44) (2009) 2093–2101, http://dx.doi.org/10.1016/j.jnoncrysol.2009.06.033.

Structural and optical characteristics

ORIGINALITY REPORT

%12	%7	%8	%
SIMILARITY INDEX	INTERNET SOURCES	PUBLICATIONS	STUDENT PAPERS

PRIMARY SOURCES

1	etrij.etri.re.kr Internet Source	%1
2	link.springer.com Internet Source	%1
3	G. Webster, H. G. Drickamer. " High pressure studies of luminescence efficiency and lifetime in La O S:Eu and Y O S:Eu ", The Journal of Chemical Physics, 1980 Publication	%1
4	pac.iupac.org Internet Source	%1
5	Pisarski, Wojciech A., Joanna Pisarska, Radosław Lisiecki, and Witold Ryba-Romanowski. "Sensitive optical temperature sensor based on up-conversion luminescence spectra of Er3+ ions in PbO–Ga2O3–XO2 (X=Ge, Si) glasses", Optical Materials, 2016. Publication	<%1
6	Zarifah, N.A., W.F. Lim, K.A. Matori, H.A.A. Sidek, Z.A. Wahab, N. Zainuddin, M.A. Salleh,	<%1

B.N. Fadilah, and A.N. Fauzana. "An elucidating study on physical and structural properties of 45S5 glass at different sintering temperatures", Journal of Non-Crystalline Solids, 2015.
Publication

7	Pavitra, E., G. Seeta Rama Raju, and Jae Su Yu. "Solvent interface effect on the size and crystalline nature of the GdPO4:Eu3+ nanorods", Materials Letters, 2015. Publication	<%1
8	M.H.A. Mhareb, S. Hashim, S.K. Ghoshal, Y.S.M. Alajerami, M.J. Bqoor, A.I. Hamdan, M.A. Saleh, M.K.B. Abdul Karim. "Effect of Dy 2 O 3 impurities on the physical, optical and thermoluminescence properties of lithium borate glass", Journal of Luminescence, 2016 Publication	<%1
9	research-repository.st-andrews.ac.uk Internet Source	<%1
10	Saidu, A., H. Wagiran, M.A. Saeed, Y.S.M. Alajerami, and A.B.A. Kadir. "Effect of co-doping of sodium on the thermoluminescence dosimetry properties of copper-doped zinc lithium borate glass system", Applied Radiation and Isotopes, 2016. Publication	<%1
11	Kailasam Saravana Mani, Balasubramanian	

	Murugesapandian, Werner Kaminsky, Subramaniam Parameswaran Rajendran. "Enantioselective approach towards the synthesis of spiro-indeno [1,2- b] quinoxaline pyrrolothiazoles as antioxidant and antiproliferative", Tetrahedron Letters, 2018 Publication	<%1
12	arxiv.org Internet Source	<%1
13	profdoc.um.ac.ir Internet Source	<%1
14	preview-nanoscalereslett.springeropen.com Internet Source	<%1
15	publik.tuwien.ac.at Internet Source	<%1
16	publications.ub.uni-mainz.de Internet Source	<%1
17	fac.ksu.edu.sa Internet Source	<%1
18	Lars Rebohle. "Electroluminescence Spectra", Springer Series in Materials Science, 2010 Publication	<%1
19	aip.scitation.org Internet Source	<%1
20	Alice E. Hall. "Identification and parasocial	

	relationships with characters from Star Wars: The Force Awakens.", Psychology of Popular Media Culture, 2017 Publication	<%1
21	Dousti, M. Reza, Gael Yves Poirier, and Andrea Simone Stucchi de Camargo. "Structural and spectroscopic characteristics of Eu3+-doped tungsten phosphate glasses", Optical Materials, 2015. Publication	<%1
22	dspace.cityu.edu.hk Internet Source	<%1
23	Annapureddy Siva Sesha Reddy, Adam Ingram, Mikhail G. Brik, Marek Kostrzewa et al. "Insulating characteristics of zinc niobium borate glass-ceramics", Journal of the American Ceramic Society, 2017 Publication	<%1
24	"Contents", Journal of Luminescence, 200505 Publication	<%1
25	Kh. S. Shaaban, Y. B. Saddeek. "Effect of MoO3 Content on Structural, Thermal, Mechanical and Optical Properties of (B2O3-SiO2-Bi2O3-Na2O-Fe2O3) Glass System", Silicon, 2017 Publication	<%1
	lup.lub.lu.se	

26	Internet Source	<%1
27	www.pathco.org Internet Source	<%1
28	eprints.kingston.ac.uk Internet Source	<%1
29	www.ec.ms.imperial.ac.uk Internet Source	<%1
30	dspace.library.iitb.ac.in Internet Source	<%1
31	espace.library.uq.edu.au Internet Source	<%1
32	dr.ntu.edu.sg Internet Source	<%1
33	eksperci.polsl.pl Internet Source	<%1
34	www.scientific.net Internet Source	<%1
35	Sontakke, A.D.. "Sensitized red luminescence from Bi^3^+ co-doped Eu^3^+: ZnO-B"2O"3 glasses", Physica B: Physics of Condensed Matter, 20091101 Publication	<%1
36	www.uta.edu	

	Internet Source	<%1
37	Wang, Lili, Hyeon Mi Noh, Byung Kee Moon, Sung Heum Park, Kwang Ho Kim, Jinsheng Shi, and Jung Hyun Jeong. "Dual-mode Luminescence with Broad near UV and Blue Excitation Band from Sr2CaMoO6:Sm3+ Phosphor for White LEDs", The Journal of Physical Chemistry C Publication	<%1
38	Pereira, P.F.S.. "Microwave synthesis of YAG:Eu by sol-gel methodology", Journal of Luminescence, 200710 Publication	<%1
39	M.I. Sayyed, Shams A.M. Issa, H.O. Tekin, Yasser B. Saddeek. "Comparative study of gamma-ray shielding and elastic properties of BaO–Bi 2 O 3 –B 2 O 3 and ZnO–Bi 2 O 3 –B 2 O 3 glass systems", Materials Chemistry and Physics, 2018 Publication	<%1
40	Zeng, Q.. "Luminescence properties of Sm^2^+-activated barium chloroborates", Journal of Luminescence, 200306 Publication	<%1

EXCLUDE QUOTES	OFF	EXCLUDE MATCHES	OFF
EXCLUDE BIBLIOGRAPHY	OFF		